We examined the effect of *EWS/ATF1* knockdown on *FOS* expression in human CCS cell lines to further investigate the association between *EWS/ATF1* expression and increased *FOS* expression in human CCS. Human CCS cell lines MP-CCS-SY and KAS carry the *EWS/ATF1* type 1 and type 2 fusion genes, respectively (Supplemental Figure 9, A and B). We next designed a specific siRNA targeting the breakpoint of the *EWS/ATF1* type 1 fusion gene, which had no effect on the expression of *ATF1* or of the *EWS/ATF1* type 2 fusion gene in KAS (Supplemental Figure 9, E and F). siRNA treatment targeting *EWS/ATF1* type 1 in MP-CCS-SY led to significant downregulation of *FOS* 48 hours after treatment (Supplemental Figure 9G) as well as of *EWS/ATF1* type 1 itself (Supplemental Figure 9, C and D), which indicates that *FOS* is a direct target of EWS/ATF1 in human CCS. In contrast to *FOS*, we observed a modest reduction of *MITF-M* expression after *EWS/ATF1* knockdown in MP-CCS-SY cells (Supplemental Figure 9H).

FOS could be a promising therapeutic target for human CCS. To examine whether *Fos* overexpression facilitates proliferation of tumor cells expressing *EWS/ATF1*, we knocked down *Fos* in *EWS/ATF1*-induced tumor cells using siRNA. The G1297 cell line was treated with siRNA for *Fos* in the presence of doxycycline. siRNA treatment (10 nM) decreased the expression of *Fos* at the mRNA level by 75% at 24 hours after transfection, although it had no effect on expression of the *EWS/ATF1* transgene compared with the control siRNA (Supplemental Figure 10A). In addition, we confirmed that Fos protein levels were also decreased 48 hours after transfection (Supplemental Figure 10B). A WST-8 assay was performed in *EWS/ATF1*-induced tumor cells transfected with the nonfunctional control siRNA or with functional *Fos* siRNA to examine the effect of *Fos* knockdown on the cellular kinetics. The siRNA targeting *Fos* efficiently inhibited cell proliferation of *EWS/ATF1*-induced tumor cells, even in the presence of doxycycline (Figure 6A). In order to further confirm the importance of *Fos* expression for *EWS/ATF1*-induced tumor cell growth, we established *EWS/ATF1*-induced tumor cell lines in which *Fos* is overexpressed (Figure 6B). We found that *Fos*-overexpressed *EWS/ATF1*-inducible cells retained the ability to proliferate for at least 48 hours after doxycycline withdrawal, whereas control cells in which *GFP* is overexpressed stopped their proliferation soon after withdrawal (Figure 6C). We also examined the effect of *FOS* knockdown on cell growth of human CCS cell lines using siRNA targeting *FOS*. Consistent with the results in *EWS/ATF1*-induced tumor cells, siRNA treatment strongly suppressed the growth of CCS cell lines (Figure 6, D and E, and Supplemental Figure 11, A–F). Taken together, these data suggest that *FOS*, a direct target of EWS/ATF1, mediates the oncogenic growth of *EWS/ATF1*-related sarcomas and could be a potent therapeutic target for human CCS.

Discussion

The current study revealed that forced expression of the *EWS/ATF1* fusion gene induced sarcoma formation in *EWS/ATF1* transgenic mice. The histology of the tumors in *EWS/ATF1* transgenic mice showed a striking similarity to that of human CCS. In addition, immunohistochemistry demonstrated that *EWS/ATF1*-induced tumor cells express neural crest–associated markers, such as S100, Mitf, and Sox10, which are also expressed in human CCS. Given that the *EWS/ATF1* fusion gene is detected in CCS, our *EWS/ATF1* transgenic mouse is the first mouse model for investigating CCS pathogenesis. Our present results demonstrated that continuous expression of *EWS/ATF1* was required for growth and tumor formation of *EWS/ATF1*-induced tumor cells. These results indicate that *EWS/ATF1* plays a pivotal role in both development and maintenance of *EWS/ATF1*-associated sarcomas, implying that CCS exhibits oncogene addiction (36) to *EWS/ATF1*, and provide a rationale for targeting EWS/ATF1 itself to treat CCS.

It is interesting to note that sarcoma formation was observed only in deep soft tissue, although *EWS/ATF1* was induced in a variety of cell types in this experimental system (37, 38). In addition, the cell proliferation rate of MEFs in vitro was reduced by *EWS/ATF1* induction. These results clearly demonstrated that the abnormal proliferation by the forced expression of *EWS/ATF1* requires a specific cell type of origin, accompanied by a specific microenvironment. Consistent with these findings, recent studies of other sarcoma-related genes revealed that introduction of *SYT/SSX*, a synovial sarcoma-related gene, into *Myf5*-positive immature myoblasts specifically resulted in sarcoma formation, whereas its expression in more differentiated cells induced myopathy without tumor induction (39). In addition, introduction of *EWS/FLI1*, a fusion gene detectable in Ewing sarcomas, results in transformation specifically in bone marrow–derived mesenchymal progenitor cells in vitro (40). Taken together, these findings are suggestive of cell type–specific carcinogenesis by expression of sarcoma-related fusion oncogenes.

Our lineage-tracing experiments in vivo suggested that *EWS/ATF1*-associated tumor cells are derived from neural crest–derived cells. This result is consistent with several lines of evidence that CCS often shows melanocytic differentiation and resembles MM. However, our present results do not exclude the possibility that *EWS/ATF1*-induced tumors can arise from non–neural crest-derived cells. In addition, the exact cell type of origin of *EWS/ATF1*-induced tumors remains unclear, since neural crest–lineage progenitors can differentiate into many different cell types, such as neuronal cells, melanocytes, and Schwann cells. Recently, Schwann cell precursors along the peripheral nerve have been shown to be a cellular source of large numbers of melanocytes in the skin during development in mice and chicks (41). Moreover, Schwann cells also retain the potential to differentiate into melanocytes, resulting from a loss of nerve contact (41). Given the finding that *EWS/ATF1*-induced tumor cells expressed markers for melanocytic differentiation, it is possible that the neural crest–derived Schwann cells could be the origin of *EWS/ATF1*-associated sarcomas.

We found that *Fos* was one of the direct targets of EWS/ATF1 in *EWS/ATF1*-induced tumor cells. *Fos* is an immediate early gene that can be activated by a variety of mitogens and growth factors. The present study showed that *Fos* induction by forced expression of *EWS/ATF1* was independent of the ERK signaling pathway. In contrast, we found that *Fos* upregulation was mediated by a CRE of the *Fos* promoter, accompanied by direct interaction of EWS/ATF1 with the CRE on the *Fos* promoter. The direct interaction of EWS/ATF1 at CRE may induce continuous transcriptional activation of *Fos* in *EWS/ATF1*-induced tumor cells. Previous studies have demonstrated a higher expression level of *FOS* to be involved in tumor growth in several cancers (42–44), and overexpression of *Fos* results in osteosarcoma formation in transgenic mice (45, 46). Here we showed that *FOS* was also upregulated in CCS by the *EWS/ATF1* fusion transcript and that the increased *FOS* promoted the growth of *EWS/ATF1*-related sarcomas. Accordingly, blocking the FOS pathway might be a promising therapeutic strategy for treating CCS (Supplemental Figure 12).

Methods

Molecular cloning and gene targeting in ES cells. Human *EWS/ATF1*-FLAG-HA was amplified by RT-PCR from the human CCS cell line KAS using primers ACATGGCGTCCACGGATTACAG and CCTAGGCGTAGTCGGGCACGTCGTAGGGGTATCCTCCAGCGGCCGACTTGTCATCGTCGTCCTTGTAGTCTCCTCCAACACTTTTATTGGAATAAAGAT and cloned into pcr2.1-TOPO. Sequence-verified *EWS/ATF1*-FLAG-HA cDNA was subcloned into a unique *EcoRI* site of pBS31 prime (37, 38). KH2 ES cells (obtained from Open Biosystems) were used to insert a single copy of *EWS/ATF1*-FLAG-HA by Flipase (PLP) recombination into the *Col1A1* locus under the control of a minimal CMV tetracycline-inducible promoter using a previously described method (37), and ES cells were selected for hygromycin resistance.

Mouse generation. For blastocyst injections, fertilized zygotes were isolated from the oviducts of day-0.5 pregnant B6D2F1 females and allowed to develop to the blastocyst stage in culture. 7–12 ES cells were injected per blastocyst. The injected blastocysts were transferred into day-2.5 pseudopregnant recipient females.

Doxycycline treatment. 6-week-old mice were administered 50 μg/ml doxycycline (Sigma-Aldrich) in their drinking water supplemented with 2 mg/ml sucrose. For cultured cells, doxycycline was used at a concentration of 0.05–0.2 μg/ml.

RNA preparation and RT-PCR. Total RNA was isolated using a RNeasy mini kit (Qiagen). Total RNA was reverse transcribed using a High-Capacity cDNA Reverse Transcription Kit with RNase inhibitor (Applied Biosystems). qRT-PCR analysis using the fluorescent SYBR green method (Bio-Rad) was performed in accordance with the manufacturer's instructions. The data generated from each reaction were subjected to gene expression analysis using an iCycler iQ Real-Time PCR Detection System (Bio-Rad). See Supplemental Table 1 for specific primer pairs used for amplification. Microarray analysis was performed with SurePrint G3 Mouse GE 8X60K microarray (Agilent Technologies) and Mouse Gene 1.0 ST Array (Affymetrix) according to the manufacturer's instructions. All analyses were performed by Genespring GX (version 12; Agilent Technologies).

Western blot analysis. Western blot analyses were carried out as described previously (47, 48). The following antibodies were used: anti-HA (rabbit IgG, 1:1,000 dilution; Cell Signaling), anti-Fos (rabbit IgG, 1:1,000 dilution; Cell Signaling), anti-ERK1/2 (rabbit IgG, 1:1,000 dilution; Cell Signaling), anti–phospho-ERK1/2 (rabbit IgG, 1:1,000 dilution; Cell Signaling), anti-ATF1 (rabbit IgG, 1:5,000 dilution; EPITOMICS), and anti-β-actin (mouse IgG, 1:5,000 dilution; Calbiochem).

Cell proliferation assay. Cell growth was determined by WST-8 assay using a Cell Counting Kit-8 (Dojindo Laboratories). Absorbance at 450 nm is indicative of the die amount of formazan, which is directly proportional to the number of living cells.

Histological analysis. Normal and tumor tissue samples were fixed in 10% buffered formalin for 24 hours and embedded in paraffin. 4-μm sections were stained with H&E, and serial sections were used for immunohistochemical analyses. Immunostaining was performed using an avidin-biotin immunoperoxidase assay. The primary antibodies used were anti-HA-Tag (1:600 dilution; Cell Signaling), anti-Ki67 (1:250 dilution; Dako), anti-S100 (1:800 dilution; Dako), anti-SOX10 (1:200 dilution; R&D Systems), anti-MITF (1:500 dilution; Exalpha), and anti-GFP (1:1,000 dilution; Abcam).

X-gal staining. Briefly, tumor tissue samples were embedded in OCT compound and frozen. 8-μm cryostat sections were immediately fixed in 0.2% glutalaldehyde for 10 minutes. The sections were stained overnight in an X-gal staining solution, then counterstained with fast red for 3 minutes.

Tumorigenicity studies. 4-week-old male BALB/c athymic mice were obtained from Japan SLC. A total of 5.0×10^6 G1297 cells in 0.1 ml serum-free DMEM was inoculated subcutaneously through a 26-gauge needle into the posterior flank of each mouse. 3 weeks after inoculation, the tumor diameters were measured with digital calipers, and tumor volume was calculated as $(w^2 \times l)/2$ and expressed in mm^3.

siRNA transfection. We performed transient knockdown assays with a siRNA targeting *Fos* (Santa Cruz), *FOS* (Santa Cruz and Dharmacon) or the breakpoint of *EWS/ATF1* type 1 (sense, GCGGUGGAAUGGGAAAAAUTT; antisense, AUUUUUCCCAUUCCACCGCTT; KOKEN) using Lipofectamine RNAiMAX (Invitrogen). We used nontargeting siRNA (Cosmo Bio Co.) as a control.

Cell lines. MP-CCS-SY and KAS are CCS cell lines carrying *EWS/ATF1* type 1 and type 2, respectively. MP-CCS-SY was established as described previously (49), and KAS was provided by T. Nakamura (Cancer Institute, Japanese Foundation for Cancer Research, Tokyo, Japan; ref. 24). HOS (osteosarcoma), U2OS (osteosarcoma), NIH3T3 (embryonic fibroblast), and WI38 (lung fibroblast) cells were purchased from the American Type Culture Collection. B16-F1 (mouse melanoma) and A375 (human MM) were purchased from the European Collection of Cell Cultures.

Mice. Wnt1-Cre mice were provided by S. Iseki (Tokyo Medical and Dental University, Tokyo, Japan; ref. 50), *P0-Cre* mice were provided by K. Yamamura (Kumamoto University, Kumamoto, Japan; ref. 51), and floxed *LacZ* mice were provided by M. Okabe (Osaka University, Suita, Japan; ref. 52). Floxed *EYFP* mice (53) were obtained from Jackson Laboratory.

Construction of the reporter plasmid. To obtain the *Fos* reporter plasmid (pGL3A-1486), the genomic DNA fragment containing −450 to +0 of the 5′-flanking sequence was amplified by PCR with the primer set 5′-TCTATCGATAGGTACGAATGTTCGCTCGCCTTCTC-3′ and 5′-ACGCGTAAGAGCTCGGGAGTAGTAGGCGCCTCAGC-3′ and subcloned into the *KpnI* site of the pGL3 vector (Promega). The *Fos* reporter plasmid with mutant CRE element was generated by PCR-targeted mutagenesis with the primer set 5′-CCAGTTCCGCCCACTCAGCTAGGAAGTCCATCC-3′ and 5′-GGATGGACTTCCTAGCTGAGTGGGCGGAACTGG-3′.

Luciferase assay. Reporter genes were transfected into the G1297 *EWS/ATF1*-induced tumor cell line together with phRL-SV40 (Promega) using lipofectamine LTX (Invitrogen), and luciferase activity was measured with a luminometer (VERITAS; Promega). Firefly luciferase activities, derived from each reporter construct, were normalized to Renilla luciferase activities from phRL-SV40.

Stable transfection. To obtain *Fos* expression plasmid (pCAG-Fos-IZ vector), *Fos* cDNA was amplified by RT-PCR from the G1297 cell line with the primer set 5′-ACATGATGTTCTCGGGTTTCAA-3′ and 5′-ACTCACAGGGCCAGCAGCGTGG-3′ and subcloned into the *ECoR* site of the pCAG-*EGFP*-IZ vector (provided by H. Niwa, RIKEN, Kobe, Japan). pCAG-*EGFP*-IZ vector or pCAG-*Fos*-IZ vector was transfected into the G1297 cell line using Lipofectamine LTX Reagent (Invitrogen) and selected for Zeocine resistance (600 μg/ml).

Patients and tumor tissue collection. Anonymized tumor specimens were obtained by surgical resection or biopsy at Gifu University Hospital or Kyoto University Hospital in accordance with an approved protocol from the Institutional Review Board. Total RNA was isolated using a RNeasy mini kit (Qiagen).

ChIP analysis. A total of 5.0×10^6 *EWS/ATF1*-inducible tumor cells was fixed in 1% formaldehyde for 10 minutes, followed by treatment with 1 ml glycine buffer for 5 minutes. Cells were pelleted, washed, and then resuspended in lysis buffer for 30 minutes. After centrifugation, the pellet was resuspended in NP40 buffer with protease inhibitors (Sigma-Aldrich). Sonication was performed using a XL-2000 (MISONIX), after which the supernatant was used as the input sample for immunoprecipitation experiments. Antibodies used were rabbit HA (Cell Signaling) and rabbit normal IgG (Abcam). Protein G–coated magnetic beads were used to purify specific antibody/DNA complexes. After washes, immunoprecipitated DNA was decrosslinked by elu-

tion buffer at 65°C for 12 hours. To remove protein and RNA, samples were incubated with RNaseA for 1 hour at 37°C and proteinase K treatment for 1 hour at 37°C. Samples were purified by PCR purification kit (Qiagen). The amount of DNA immunoprecipitated with HA-tagged protein was quantified by real-time PCR with primers flanking the *Fos* promoter, including the CRE element (forward, 5′-TCCTACACGCGGAAGGTCTAGG-3′; reverse, 5′-TAGAAGCGCTGTGAATGGATGG-3′). Primers 5′-GCACTAATTAGTCGCGGTGGTGG-3′ (forward) and 5′-CAGGGTCTTAGTGGGATCAAGG-3′ (reverse) were used as a negative control.

Accession number. The profiling data cited in Supplemental Figure 6 are available at GEO (accession no. GSE41123).

Statistics. Statistical analyses were carried out using GraphPad Prism (version 5.01; GraphPad Software). Data were analyzed using ANOVA, and *P* values less than 0.05 were considered statistically significant.

Study approval. Animal experiments were approved by the Gifu University Animal Experiment Committee, and the care of the animals was in accordance with institutional guidelines. All clinical samples were approved for analysis by the Ethics Committee at Kyoto University Graduate School and Faculty of Medicine (Kyoto, Japan). Written informed consent was obtained from all patients with cancers analyzed in this study.

Acknowledgments

The authors thank K. Woltjen and T. Yamamoto (CiRA, Kyoto University) for careful reading of the manuscript and helpful comments. We also thank T. Motohashi (Tissue and Organ Development Regeneration and Advanced Medical Science) for helpful discussion and the members of the Department of Orthopedic Surgery and Department of Tumor Pathology, Gifu University Graduate School of Medicine; the Department of Orthopaedic Surgery, Graduate School of Medicine, Kyoto University; and the Toguchida and Yamada laboratories for their valuable technical assistance. This study was supported by grants from the Ministry of Education, Culture, Sports, Science, and Technology of Japan and from the Ministry of Health, Labor, and Welfare of Japan.

Received for publication February 28, 2012, and accepted in revised form November 1, 2012.

Address correspondence to: Yasuhiro Yamada, Center for iPS Cell Research and Application (CiRA), Institute for Integrated Cell-Material Sciences (WPI-iCeMS), Kyoto University, 53 Kawahara-cho, Shogoin, Sakyo-ku, Kyoto 606-8507, Japan. Phone: 81.75.366.7034; Fax: 81.75.366.7093; E-mail: y-yamada@cira.kyoto-u.ac.jp. Or to: Takatoshi Ohno, Department of Orthopaedic Surgery, Gifu University Graduate School of Medicine, 1-1 Yanagido, Gifu 501-1194, Japan. Phone: 81.58.230.6333; Fax: 81.58.230.6334; E-mail: takaohno@gifu-u.ac.jp.

1. Enzinger FM. Clear-cell sarcoma of tendons and aponeuroses. An analysis of 21 cases. *Cancer*. 1965; 18:1163–1174.
2. Covinsky M, Gong S, Rajaram V, Perry A, Pfeifer J. EWS-ATF1 fusion transcripts in gastrointestinal tumors previously diagnosed as malignant melanoma. *Hum Pathol*. 2005;36(1):74–81.
3. Deenik W, Mooi WJ, Rutgers EJ, Peterse JL, Hart AA, Kroon BB. Clear cell sarcoma (malignant melanoma) of soft parts: A clinicopathologic study of 30 cases. *Cancer*. 1999;86(6):969–975.
4. Ferrari A, et al. Clear cell sarcoma of tendons and aponeuroses in pediatric patients: a report from the Italian and German Soft Tissue Sarcoma Cooperative Group. *Cancer*. 2002;94(12):3269–3276.
5. Finley JW, Hanypsiak B, McGrath B, Kraybill W, Gibbs JF. Clear cell sarcoma: the Roswell Park experience. *J Surg Oncol*. 2001;77(1):16–20.
6. Eckardt JJ, Pritchard DJ, Soule EH. Clear cell sarcoma. A clinicopathologic study of 27 cases. *Cancer*. 1983;52(8):1482–1488.
7. Kawai A, et al. Clear cell sarcoma of tendons and aponeuroses: a study of 75 patients. *Cancer*. 2007;109(1):109–116.
8. Kindblom LG, Lodding P, Angervall L. Clear-cell sarcoma of tendons and aponeuroses. An immunohistochemical and electron microscopic analysis indicating neural crest origin. *Virchows Arch A Pathol Anat Histopathol*. 1983;401(1):109–128.
9. Segal NH, et al. Classification of clear-cell sarcoma as a subtype of melanoma by genomic profiling. *J Clin Oncol*. 2003;21(9):1775–1781.
10. Bridge JA, Borek DA, Neff JR, Huntrakoon M. Chromosomal abnormalities in clear cell sarcoma. Implications for histogenesis. *Am J Clin Pathol*. 1990; 93(1):26–31.
11. Bridge JA, Sreekantaiah C, Neff JR, Sandberg AA. Cytogenetic findings in clear cell sarcoma of tendons and aponeuroses. Malignant melanoma of soft parts. *Cancer Genet Cytogenet*. 1991;52(1):101–106.
12. Sandberg AA, Bridge JA. Updates on the cytogenetics and molecular genetics of bone and soft tissue tumors: clear cell sarcoma (malignant melanoma of soft parts). *Cancer Genet Cytogenet*. 2001;130(1):1–7.
13. Kim J, Lee K, Pelletier J. The DNA binding domains of the WT1 tumor suppressor gene product and chimeric EWS/WT1 oncoprotein are functionally distinct. *Oncogene*. 1998;16(8):1021–1030.
14. Lessnick SL, Braun BS, Denny CT, May WA. Multiple domains mediate transformation by the Ewing's sarcoma EWS/FLI-1 fusion gene. *Oncogene*. 1995;10(3):423–431.
15. Pan S, Ming KY, Dunn TA, Li KK, Lee KA. The EWS/ATF1 fusion protein contains a dispersed activation domain that functions directly. *Oncogene*. 1998;16(12):1625–1631.
16. Ohno T, Ouchida M, Lee L, Gatalica Z, Rao VN, Reddy ES. The EWS gene, involved in Ewing family of tumors, malignant melanoma of soft parts and desmoplastic small round cell tumors, codes for an RNA binding protein with novel regulatory domains. *Oncogene*. 1994;9(10):3087–3097.
17. Petermann R, Mossier BM, Aryee DN, Khazak V, Golemis EA, Kovar H. Oncogenic EWS-Fli1 interacts with hsRPB7, a subunit of human RNA polymerase II. *Oncogene*. 1998;17(5):603–610.
18. Gonzalez GA, Montminy MR. Cyclic AMP stimulates somatostatin gene transcription by phosphorylation of CREB at serine 133. *Cell*. 1989;59(4):675–680.
19. Comb M, Birnberg NC, Seasholtz A, Herbert E, Goodman HM. A cyclic AMP- and phorbol ester-inducible DNA element. *Nature*. 1986; 323(6086):353–356.
20. Montminy MR, Sevarino KA, Wagner JA, Mandel G, Goodman RH. Identification of a cyclic-AMP-responsive element within the rat somatostatin gene. *Proc Natl Acad Sci U S A*. 1986;83(18):6682–6686.
21. Li KK, Lee KA. MMSP tumor cells expressing the EWS/ATF1 oncogene do not support cAMP-inducible transcription. *Oncogene*. 1998;16(10):1325–1331.
22. Brown AD, Lopez-Terrada D, Denny C, Lee KA. Promoters containing ATF-binding sites are de-regulated in cells that express the EWS/ATF1 oncogene. *Oncogene*. 1995;10(9):1749–1756.
23. Fujimura Y, Ohno T, Siddique H, Lee L, Rao VN, Reddy ES. The EWS-ATF-1 gene involved in malignant melanoma of soft parts with t(12;22) chromosome translocation, encodes a constitutive transcriptional activator. *Oncogene*. 1996;12(1):159–167.
24. Jishage M, Fujino T, Yamazaki Y, Kuroda H, Nakamura T. Identification of target genes for EWS/ATF-1 chimeric transcription factor. *Oncogene*. 2003; 22(1):41–49.
25. Davis IJ, et al. Oncogenic MITF dysregulation in clear cell sarcoma: defining the MiT family of human cancers. *Cancer Cell*. 2006;9(6):473–484.
26. Antonescu CR, Tschernyavsky SJ, Woodruff JM, Jungbluth AA, Brennan MF, Ladanyi M. Molecular diagnosis of clear cell sarcoma: detection of EWS-ATF1 and MITF-M transcripts and histopathological and ultrastructural analysis of 12 cases. *J Mol Diagn*. 2002;4(1):44–52.
27. Granter SR, Weilbaecher KN, Quigley C, Fletcher CD, Fisher DE. Clear cell sarcoma shows immunoreactivity for microphthalmia transcription factor: further evidence for melanocytic differentiation. *Mod Pathol*. 2001;14(1):6–9.
28. Li KK, et al. The melanocyte inducing factor MITF is stably expressed in cell lines from human clear cell sarcoma. *Br J Cancer*. 2003;89(6):1072–1078.
29. Levy C, Khaled M, Fisher DE. MITF: master regulator of melanocyte development and melanoma oncogene. *Trends Mol Med*. 2006;12(9):406–414.
30. Garraway LA, et al. Integrative genomic analyses identify MITF as a lineage survival oncogene amplified in malignant melanoma. *Nature*. 2005; 436(7047):117–122.
31. Speleman F, Delattre O, Peter M, Hauben E, Van Roy N, Van Marck E. Malignant melanoma of the soft parts (clear-cell sarcoma): confirmation of EWS and ATF-1 gene fusion caused by a t(12;22) translocation. *Mod Pathol*. 1997;10(5):496–499.
32. Jiang X, Rowitch DH, Soriano P, McMahon AP, Sucov HM. Fate of the mammalian cardiac neural crest. *Development*. 2000;127(8):1607–1616.
33. Setternes OM, Sorensen R, Johansen B, Loennechen T, Aarbakke J, Moens U. Synergistic increase in c-fos expression by simultaneous activation of the ras/raf/map kinase- and protein kinase A signaling pathways is mediated by the c-fos AP-1 and SRE sites. *Biochim Biophys Acta*. 1998;1395(3):345–360.
34. Ginty DD, Bonni A, Greenberg ME. Nerve growth factor activates a Ras-dependent protein kinase that stimulates c-fos transcription via phosphorylation of CREB. *Cell*. 1994;77(5):713–725.
35. Sassone-Corsi P, Visvader J, Ferland L, Mellon PL, Verma IM. Induction of proto-oncogene fos transcription through the adenylate cyclase pathway:

characterization of a cAMP-responsive element. *Genes Dev.* 1988;2(12A):1529–1538.
36. Weinstein IB. Cancer. Addiction to oncogenes – the Achilles heal of cancer. *Science.* 2002;297(5578):63–64.
37. Beard C, Hochedlinger K, Plath K, Wutz A, Jaenisch R. Efficient method to generate single-copy transgenic mice by site-specific integration in embryonic stem cells. *Genesis.* 2006;44(1):23–28.
38. Hochedlinger K, Yamada Y, Beard C, Jaenisch R. Ectopic expression of Oct-4 blocks progenitor-cell differentiation and causes dysplasia in epithelial tissues. *Cell.* 2005;121(3):465–477.
39. Haldar M, Hancock JD, Coffin CM, Lessnick SL, Capecchi MR. A conditional mouse model of synovial sarcoma: insights into a myogenic origin. *Cancer Cell.* 2007;11(4):375–388.
40. Riggi N, et al. Development of Ewing's sarcoma from primary bone marrow-derived mesenchymal progenitor cells. *Cancer Res.* 2005;65(24):11459–11468.
41. Adameyko I, et al. Schwann cell precursors from nerve innervation are a cellular origin of melanocytes in skin. *Cell.* 2009;139(2):366–379.
42. Guller M, et al. c-Fos overexpression increases the proliferation of human hepatocytes by stabilizing nuclear Cyclin D1. *World J Gastroenterol.* 2008; 14(41):6339–6346.
43. Pandey MK, Liu G, Cooper TK, Mulder KM. Knockdown of c-Fos suppresses the growth of human colon carcinoma cells in athymic mice. *Int J Cancer.* 2012;130(1):213–222.
44. Saez E, et al. c-fos is required for malignant progression of skin tumors. *Cell.* 1995;82(5):721–732.
45. Grigoriadis AE, Schellander K, Wang ZQ, Wagner EF. Osteoblasts are target cells for transformation in c-fos transgenic mice. *J Cell Biol.* 1993; 122(3):685–701.
46. Wang ZQ, Grigoriadis AE, Mohle-Steinlein U, Wagner EF. A novel target cell for c-fos-induced oncogenesis: development of chondrogenic tumours in embryonic stem cell chimeras. *EMBO J.* 1991;10(9):2437–2450.
47. Nozawa S, et al. Inhibition of platelet-derived growth factor-induced cell growth signaling by a short interfering RNA for EWS-Fli1 via down-regulation of phospholipase D2 in Ewing sarcoma cells. *J Biol Chem.* 2005;280(30):27544–27551.
48. Yamamoto T, et al. Simultaneous inhibition of mitogen-activated protein kinase and phosphatidylinositol 3-kinase pathways augment the sensitivity to actinomycin D in Ewing sarcoma. *J Cancer Res Clin Oncol.* 2009;135(8):1125–1136.
49. Moritake H, et al. Newly established clear cell sarcoma (malignant melanoma of soft parts) cell line expressing melanoma-associated Melan-A antigen and overexpressing C-MYC oncogene. *Cancer Genet Cytogenet.* 2002;135(1):48–56.
50. Chai Y, et al. Fate of the mammalian cranial neural crest during tooth and mandibular morphogenesis. *Development.* 2000;127(8):1671–1679.
51. Yamauchi Y, et al. A novel transgenic technique that allows specific marking of the neural crest cell lineage in mice. *Dev Biol.* 1999;212(1):191–203.
52. Sakai K, Miyazaki J. A transgenic mouse line that retains Cre recombinase activity in mature oocytes irrespective of the cre transgene transmission. *Biochem Biophys Res Commun.* 1997;237(2):318–324.
53. Srinivas S, et al. Cre reporter strains produced by targeted insertion of EYFP and ECFP into the ROSA26 locus. *BMC Dev Biol.* 2001;1:4.

Journal of Dental Research
http://jdr.sagepub.com/

Hypoxia-enhanced Derivation of iPSCs from Human Dental Pulp Cells

K. Iida, T. Takeda-Kawaguchi, M. Hada, M. Yuriguchi, H. Aoki, N. Tamaoki, D. Hatakeyama, T. Kunisada, T. Shibata and K. Tezuka

J DENT RES 2013 92: 905 originally published online 20 August 2013
DOI: 10.1177/0022034513502204

The online version of this article can be found at:
http://jdr.sagepub.com/content/92/10/905

Published by:
SAGE
http://www.sagepublications.com

On behalf of:
International and American Associations for Dental Research

>> Version of Record - Sep 16, 2013

OnlineFirst Version of Record - Aug 20, 2013

What is This?

RESEARCH REPORTS
Biological

K. Iida[1], T. Takeda-Kawaguchi[1], M. Hada[2], M. Yuriguchi[2], H. Aoki[2], N. Tamaoki[1], D. Hatakeyama[1], T. Kunisada[2], T. Shibata[1], and K. Tezuka[2]*

[1]Department of Oral and Maxillofacial Science, Gifu University Graduate School of Medicine, 1-1 Yanagido, Gifu City, Gifu 501-1194, Japan; and [2]Department of Tissue and Organ Development, Gifu University Graduate School of Medicine, 1-1 Yanagido, Gifu City, Gifu 501-1194, Japan; *corresponding author, tezuka@gifu-u.ac.jp

J Dent Res 92(10):905-910, 2013

Hypoxia-enhanced Derivation of iPSCs from Human Dental Pulp Cells

ABSTRACT

Hypoxia enhances the reprogramming efficiency of human dermal fibroblasts to become induced pluripotent stem cells (iPSCs). Because we showed previously that hypoxia facilitates the isolation and maintenance of human dental pulp cells (DPCs), we examined here whether it promotes the reprogramming of DPCs to become iPSCs. Unlike dermal fibroblasts, early and transient hypoxia (3% O_2) induced the transition of DPCs to iPSCs by 3.3- to 5.1-fold compared with normoxia (21% O_2). The resulting iPSCs closely resembled embryonic stem cells as well as iPSCs generated in normoxia, as judged by morphology and expression of stem cell markers. However, sustained hypoxia strongly inhibited the appearance of iPSC colonies and altered their morphology, and antioxidants failed to suppress this effect. Transient hypoxia increased the expression levels of *NANOG* and *CDH1* and modulated the expression of numerous genes, including those encoding chemokines and their receptors. Therefore, we conclude that hypoxia, when optimized for cell type, is a simple and useful tool to enhance the reprogramming of somatic cells to become iPSCs.

KEY WORDS: cell hypoxia, stem cells, odontoblasts, cadherins, microarray analysis, chemokines.

DOI: 10.1177/0022034513502204

Received April 9, 2013; Last revision July 19, 2013; Accepted July 30, 2013

A supplemental appendix to this article is published electronically only at http://jdr.sagepub.com/supplemental.

INTRODUCTION

Human dental pulp cells (DPCs) are present in dental pulp tissues, and function as stem/progenitor cells through their ability to self-renew and differentiate into restricted-lineages (Gronthos *et al.*, 2000, 2002; Takeda *et al.*, 2008). We previously reported that retroviral transduction of 4 transcription factors (*OCT3/4, SOX2, KLF4*, and *c-MYC*) can reprogram DPCs into induced pluripotent stem cells (iPSCs) that closely resemble embryonic stem cells (ESCs). These findings suggested that an iPSC bank can be established from DPCs as a valuable resource for regenerative medicine (Tamaoki *et al.*, 2010; Okita *et al.*, 2011). However, dental pulp tissues isolated from aged donors (45-68 yrs) are smaller, form fewer DPC colonies in culture, and have diminished proliferative capacity (Iida *et al.*, 2010). Therefore, to establish iPSCs from a wide range of donors, such as patients with chronic diseases specific to later stages of life, it is important to improve reprogramming and colony-forming efficiencies of primary cultures.

Human peripheral tissues reside in a low-oxygen-tension environment. Therefore, low-oxygen tension is suitable for establishing and maintaining human somatic cells (Packer and Fuehr, 1977; D'Ippolito *et al.*, 2006). Rat incisor pulp tissue is surrounded by hard dentin tissue, and its oxygen tension (23.2 mm Hg, 3% O_2) is lower than that of air (Yu *et al.*, 2002). We previously showed that hypoxia (3% O_2) enhances proliferation and inhibits differentiation of human DPCs (Iida *et al.*, 2010). Recently, exposure to hypoxia was reported to enhance the reprogramming of human dermal fibroblast cells (DFs) (Yoshida *et al.*, 2009). Therefore, we reasoned that hypoxia might enhance the reprogramming of DPCs toward iPSCs. Thus, the goal of the present study was to test the effect of hypoxia on reprogramming human DPCs.

MATERIALS & METHODS

Cell Culture and Generation of iPSCs

Human DPCs, collected from patients at Gifu University Hospital who provided informed consent, were isolated and cultured by previously reported techniques (Gronthos *et al.*, 2000) and modifications as described in the Appendix. Following the guidelines for the generation of human iPSCs approved by the Institutional Review Board of Gifu University, we used DPCs from three donors (DP31, 14-year-old girl; DP54, 19-year-old man; and

Table 1. Genes Up-regulated (Hypoxia>Normoxia) or Down-regulated (Hypoxia<Normoxia) by >5-fold

Hypoxia>Normoxia			Hypoxia<Normoxia		
Gene Symbol	GenBank Accession Number	Fold-increase	Gene Symbol	GenBank Accession Number	Fold-increase
ANKRD24	NM_133475	38.43	*CXCR3*	NM_001504	10.91
CBLC	NM_012116	30.23	*MKRN3*	NM_005664	10.65
GFRA2	NM_001495	25.99	*GTSF1*	NM_144594	7.29
ATP9A	NM_006045	17.16	*CXCL1*	NM_001511	7.22
EGLN3	NM_022073	12.33	*CPA2a*	NM_001869	7.14
SORBS1	AK022468	8.91	*RGS18*	NM_130782	6.28
ANGPTL4	NM_139314	8.88	*OLAH*	NM_001039702	6.20
LILRA3	NM_006865	8.81	*FTMT*	NM_177478	6.14
PTPRB	NM_002837	7.96	*IL8*	NM_000584	5.74
SFTPA1	NM_005411	7.95	*KRTAP3-2*	NM_031959	5.11
CCR4	NM_005508	7.38			
OCLN	NM_002538	7.12			
SMPD3	NM_018667	7.02			
CA9	NM_001216	6.45			
IGFBP3	NM_001013398	6.37			
INHBB	NM_002193	6.34			
CDH1	NM_004360	5.75			
AQP1	NM_198098	5.56			
FAM189A2	NM_004816	5.45			
MCHR1	NM_005297	5.30			
APLN	NM_017413	5.18			

DP185, 62-year-old man) for generating iPSCs within 10 passages. Using a retroviral vector, we generated iPSCs that express the transcription factors encoded by *OCT3/4, SOX2, KLF4*, and *c-MYC* according to a published protocol (Takahashi *et al.*, 2007; Tamaoki *et al.*, 2010). To determine the reprogramming efficiency of DPCs under hypoxia, we cultured these cells in atmospheres containing either 21% O_2 or 3% O_2 and analyzed them according to the time schedule described in the Appendix. At 6 days post-infection, the cells were seeded onto feeder layers (see Appendix) and cultured in 21% O_2. On day 21, we counted the number of human ESC-like colonies and alkaline phosphatase (ALP)-positive colonies and isolated total RNA from the cells to determine the level of *NANOG* expression. To characterize iPSCs, we selected ESC-like colonies from days 14 to 21 and cultured them in 21% O_2. Assays were performed in triplicate, and the values of average and standard deviation (SD) were calculated. Student's *t* test was used for determining significance. A human ESC line (KhES01) was obtained from Kyoto University (Kyoto, Japan) and cultured on mitomycin C-treated SNL feeder layers (SNL cell line obtained from Sanger Institute, Cambridge, UK) in Primate ES cell medium (ReproCell, Tokyo, Japan) supplemented with 4 ng/mL basic fibroblast growth factor (Wako, Osaka, Japan).

Quantitative Real-time Polymerase Chain-reaction (RT-PCR)

RNA extraction (RNeasy Plus Mini Kit; Qiagen, Valencia, CA, USA) and RT-PCR (Thermal Cycler Dice Real Time System TP800; Takara, Shiga, Japan) were performed as described previously (Takeda *et al.*, 2008). The mRNA data were normalized to those of *GAPDH* and used to calculate expression coefficients. Primer sequences are shown in Appendix Table 1. Primers used for *OCT3/4, SOX2*, and *KLF4* specifically detect the endogenous transcripts (Takahashi *et al.*, 2007). For comparison of the expression levels of *CDH1* (E-cadherin) and *CXCR3* in DPCs exposed to normoxia and hypoxia, DPCs from the three donors were transduced as described above or not and then cultured for 6 days under 21% O_2 or 3% O_2. Expression levels of *CDH1* and *CXCR3* mRNA were assessed by RT-PCR at day 6 post-infection.

Immunohistochemistry

The cells were fixed with 4% paraformaldehyde for 15 min and treated with phosphate-buffered saline (PBS) containing 2% normal goat or donkey serum (Wako), 0.5% BSA (Sigma-Aldrich, St. Louis, MO, USA), and 0.2% Triton X-100 (Wako) for 30 min. The primary and secondary antibodies are shown in the Appendix. Nuclei were stained with 4′,6-diamidino-2-phenylindole (DAPI) (Merck Millipore, Billerica, MA, USA).

Teratoma Formation Assays

Teratoma formation assays were performed as reported (Takahashi *et al.*, 2007; Watanabe *et al.*, 2007). Briefly, 3×10^5 iPSCs were injected by means of a Hamilton syringe into the testes of six-week-old immunodeficient nude mice (BALB/c nu/nu; CLEA, Tokyo, Japan). Twelve wks after injection, tumors were dissected and fixed with PBS containing 4% paraformal-

dehyde. Paraffin-embedded tissues were sectioned (3 μm) with a microtome (TU-213, YAMATO KOUKI, Asaka, Japan) and stained with hematoxylin and eosin.

Microarray Analysis

DPCs from three donors (DP31, DP54, and DP185) that had been induced with the reprogramming factors were cultured in atmospheres of 21% O_2 or 3% O_2, according to the time schedule for hypoxic assessment described above. Total RNA was isolated with an RNeasy Plus Mini Kit (Qiagen) on day 6 after transduction. The cDNA microarray analysis was performed as described in the Appendix. The level of gene expression was determined by use of Gene Spring GX11.5 (Agilent Technologies, Santa Clara, CA, USA). The raw microarray data are deposited in the National Center for Biotechnology Information Gene Expression Omnibus (GEO Series GSE45872; http://www.ncbi.nlm.nih.gov/geo/).

Statistical Analysis

Data are presented as the mean ± SD. The differences in mean values were evaluated by the *t* test after evaluation of variances (Microsoft Excel). For RT-PCR, the mean and standard deviation of the expression coefficient were calculated with Thermal Cycler Dice® Real Time System Software Ver. 4.02 (Takara).

RESULTS

Hypoxia Enhances Reprogramming of DPCs

With a retrovirus vector, *OCT3/4, SOX2, KLF4*, and *c-MYC* were introduced into DPCs isolated from three individuals (DP31, DP54, and DP185), and 24 hrs later the cells were cultured under hypoxia (3% O_2) for 6 days and re-plated onto SNL feeder cells in an atmosphere containing 21% O_2 for an additional 14 days. Prolonged exposure to hypoxia after passage suppressed colony formation and altered the appearance of the ESC-like colonies. These colonies either became less compact (Appendix Fig. 1A) or their morphology was altered by the presence of peripheral spindle-like cells (Appendix Fig. 1B). However, exposure of DPCs to hypoxia for only the first 6 days significantly increased the number of ALP-positive (1.9- to 3.2-fold) and ESC-like colonies (3.3- to 5.1-fold, Fig. 1A). The expression levels of *NANOG* significantly increased, suggesting that this transient hypoxia enhanced reprogramming of the cells (Fig. 1B). There was a marked increase in the ratio of ESC-like colonies to ALP-positive cells generated from DPCs from a 62-year-old donor. This time schedule differed from that used in a previous study demonstrating that exposure of human DFs to 5% O_2 for 7 to 21 days of reprogramming enhanced generation of iPSCs (Yoshida *et al.*, 2009).

To investigate why prolonged cultivation of DPCs under 3% O_2 strongly suppressed colony formation and expansion, we checked the effect of hypoxia on established DPC-derived iPSCs. The growth of iPSCs established from DPCs did not change significantly in 3% O_2, suggesting that the morphology and proliferation of iPSCs were not affected once reprogramming was completed (Appendix Fig. 1C). We next cultured DPCs

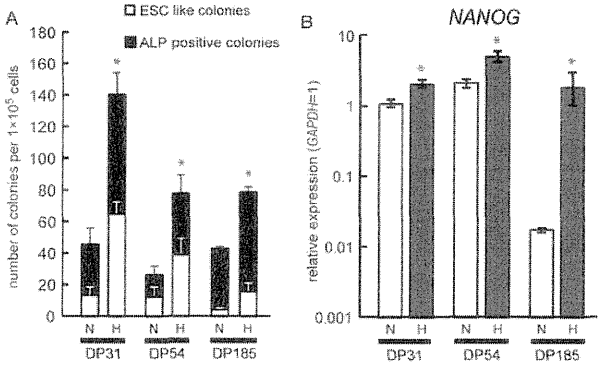

Figure 1. Generation of iPSCs under hypoxia. **(A)** Numbers of ESC-like colonies (white) and ALP-positive colonies (black) generated from 1 × 10^5 DPCs on day 21 after retroviral transduction. We transduced DPCs from three donors (DP31, DP54, and DP185) with retroviral expression vectors containing the genes encoding 4 programming factors (*OCT3/4, SOX2, KLF4*, and *c-MYC*), and incubated them in atmospheres of either 21% O_2 (N) or 3% O_2 (H) 1 to 6 days after virus infection, re-seeded them onto SNL feeder cells on day 6, and then incubated them in an atmosphere of 21% O_2. Mean numbers of colonies from 3 experiments (n = 3) are shown with error bars indicating SD; $*p < .05$ compared with 21% O_2. **(B)** The levels of *NANOG* expression were quantified by RT-PCR. Error bars indicate the SD obtained from triplicate measurements.

exposed to hypoxia for 2 days and observed increased levels of reactive oxygen species (ROS) (Appendix Fig. 2A). When DPCs were subjected to hypoxia, ROS generation was suppressed by anti-oxidants such as vitamins C and E (data not shown); however, when we generated iPSCs under 3% O_2 in the presence of these anti-oxidants for 21 days, we did not detect an increase in the induction of iPSCs (Appendix Fig. 2B), suggesting that ROS generation did not account for the adverse effects of sustained hypoxia. We conclude, therefore, that transient exposure to hypoxia at an early stage of reprogramming had a positive effect on DPCs, which was different from the effect on DFs.

The iPSC colonies were characterized by their ESC-like morphology and ALP activity (Figs. 2A, 2B, and Appendix Table 2). They were positive for OCT3/4, SSEA-4, TRA1-60, and TRA1-81, and negative for SSEA-1 (Figs. 2C-2G and Appendix Table 2). RT-PCR analysis showed that expression of *NANOG* and *REX1* was comparable with that of human ESCs, and endogenous *OCT3/4, SOX2*, and *KLF4* were also expressed (Fig. 2H). These cells also formed teratomas in nude mice, suggesting that they possess the characteristics of iPSCs (Figs. 2I-2K).

Effect of Transient Hypoxia Treatment on Gene Expression in DPCs

To assess the responses of DPCs to hypoxia, we first determined the levels of HIF-1α expression by cultures of DPCs exposed to hypoxia for 2, 4, and 24 hrs. The expression of HIF-1α increased transiently, suggesting a relatively rapid adaptation of the cells to hypoxia within 48 hrs (data not shown). To investigate the effect of oxygen concentration on global gene expression, we compared DPCs cultured for 6 days under hypoxia and normoxia (Appendix Figs. 3 and 4). Under hypoxia, the expression

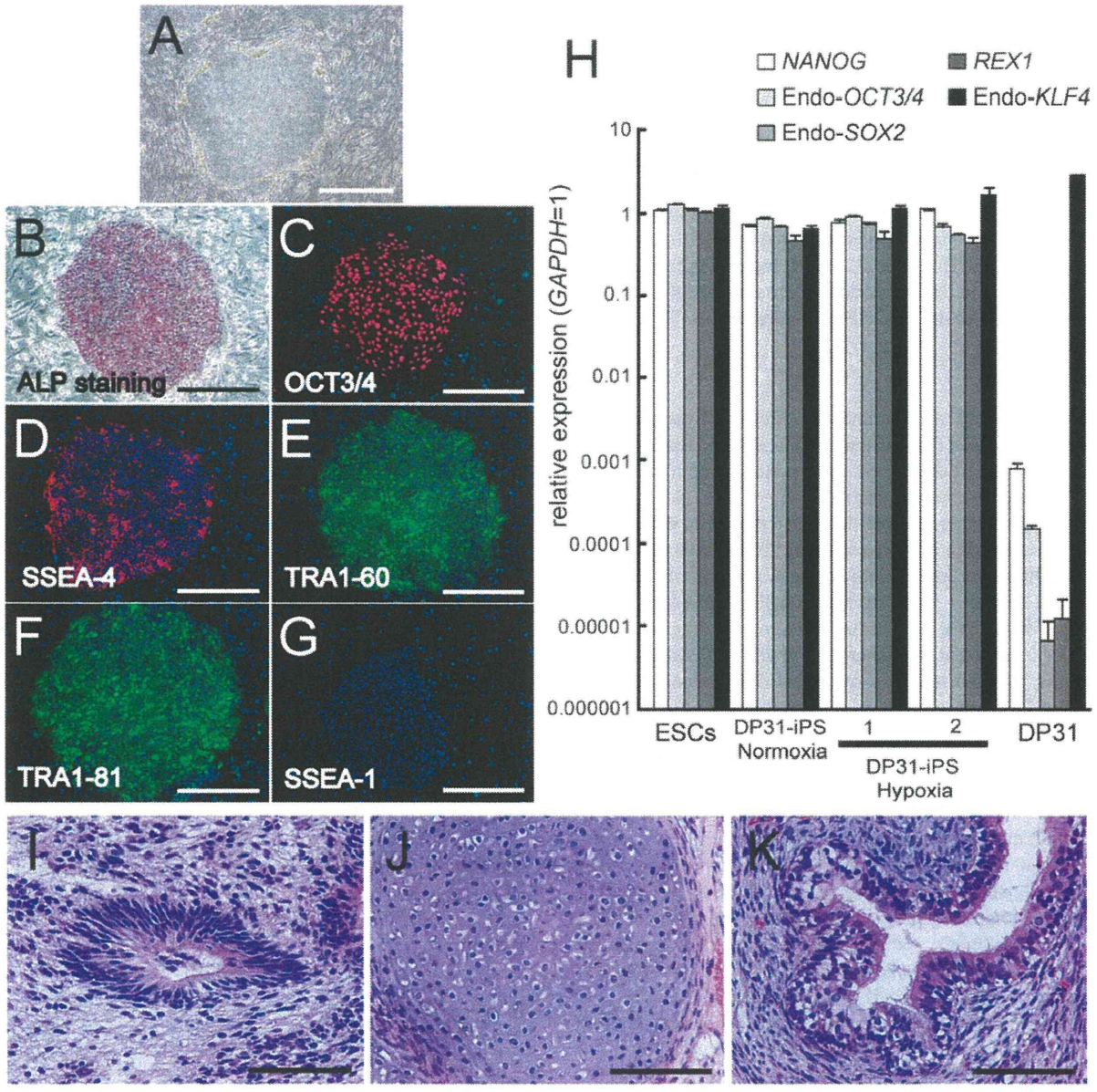

Figure 2. Characterization of iPSCs generated under hypoxic condition. **(A)** Typical morphology of an iPSC colony generated from DP31 under hypoxia (DP31-iPS-1). Scale bar = 200 μm. **(B–G)** iPSCs generated from DP31 under hypoxia (DP31-iPS-1) expressed ALP (B) and pluripotency markers OCT3/4 (C), SSEA-4 (D), TRA1-60 (E), and TRA1-81 (F), but not SSEA-1 (G), as judged by immunostaining. Nuclei were stained with DAPI. Scale bar = 200 μm. **(H)** RT-PCR analysis of ESC-marker genes in iPSCs (DP31-iPS-1 and -2) generated from DP31 under hypoxia, iPSCs generated under normoxia, human ESCs, and DP31. Numbers indicate different iPSC clones generated from DP31. Endogenous *NANOG, OCT3/4, SOX2, REX1,* and *KLF4* were expressed in 2 iPSCs lines generated under hypoxia as well as in human ESCs and iPSCs generated under normoxia, but not in DPCs. Error bars indicate the SD calculated from triplicates. **(I–K)** To confirm the pluripotency of iPSCs generated from DP31 exposed to hypoxia (DP31-iPS-1), we injected the cells into the testes of immunodeficient nude mice to generate teratomas. Twelve wks after injection, we observed tumor formation. Hematoxylin- and eosin-stained teratoma sections show that the tumor contained various types of tissues, such as neural-tube-like structures (I, ectoderm tissue), cartilage (J, mesoderm tissue), and gut-like epithelial tissues (K, endoderm tissue). Scale bar = 200 μm.

of 21 genes increased at least 5-fold (Table 1). Activation of epithelial and inhibition of mesenchymal genes (mesenchymal-epithelial transition, MET) is required for reprogramming mesenchymal cells into iPSCs (Li *et al.*, 2010). *CDH1* (E-cadherin) is an epithelial gene required for reprogramming (Chen *et al.*, 2010; Li *et al.*, 2010). Therefore, we further confirmed the expression of E-cadherin using RT-PCR, suggesting that MET was stimulated in DPCs by hypoxia (Fig. 3A). In contrast, the expression of 10 genes decreased. *CXCR3*, which encodes a chemokine receptor, was down-regulated (Fig. 3B). It should be noted that E-cadherin was significantly down-regulated in hypoxia without introduction of reprogramming factors. We

assume that hypoxia supported the MET in the presence but not the absence of reprogramming factors.

Mir-302 is predominantly expressed in human ESCs or iPSCs, mediates reprogramming of somatic cells, and is up-regulated in hypoxia (Suh *et al.*, 2004; Wilson *et al.*, 2009; Lin *et al.*, 2011; Foja *et al.*, 2013). We determined microRNA levels using microarray analyses of DPCs cultured under conditions of normoxia or hypoxia for 7 days (Appendix Table 3). Mir-302 was not detected in either case; however, Mir-210 was up-regulated over 2-fold in hypoxia, which is regulated by HIF-1α in a variety of tumor types (Huang *et al.*, 2009), suggesting that hypoxia induced changes in the expression of certain microRNAs without affecting that of the ESCs/iPSCs-specific Mir-302.

DISCUSSION

In the present study, we examined the effects of hypoxia on the generation of human iPSCs from DPCs and found that exposure to hypoxia (3% O_2) during the early period of reprogramming (days 1 to day 6) enhanced the induction of ESC-like colonies. Interestingly, when we treated the transfected cells with 3% O_2 during the later stage of reprogramming (from day 6 to day 21), these conditions strongly inhibited the generation of iPSCs. In contrast, a previous study of human DFs exposed to milder hypoxia (5% O_2) in a later period of reprogramming (days 7 to 21 or later) enhanced the generation of iPSCs (Yoshida *et al.*, 2009). Our previous reports showed that iPSC colonies derived from most DPCs lines start to appear by 14 days after retroviral transduction, but human DFs do not start to form any iPSC colonies until 21 days (Tamaoki *et al.*, 2010). Therefore, we conclude from our present findings that exposure to hypoxia from days 1 through 6 after retroviral transduction conforms to the reprogramming schedule of DPCs.

We do not know why prolonged culture under hypoxic conditions strongly inhibited colony formation and growth of maturing iPSCs at late stages of reprogramming. The proliferation of DPCs was optimum in 3% O_2, and DPCs are known to resist hypoxia in 1% O_2 (Iida *et al.*, 2010). Moreover, 3% O_2 did not affect the proliferation or morphology of established iPSCs. Therefore, we assume that hypoxia (3% O_2) may not be toxic for either DPCs or iPSCs; however, it may instead affect an unstable stage involved in their maturation. Further, although we found that the ROS levels were up-regulated in DPCs in 3% O_2, we could not rescue iPSCs from the inhibitory effects of hypoxia using anti-oxidants (Appendix Figs. 2A-2B). We predict that other factors, such as metabolic changes, may be involved.

E-cadherin is a transmembrane constituent of intercellular adherens junctions that are responsible for maintaining epithelial cohesion (Cavallaro and Christofori, 2004) and has been linked to the control of ESC pluripotency (Chou *et al.*, 2008; Soncin *et al.*, 2009). Li *et al.* (2010) reported that exogenous reprogramming factors activate an epithelial program and inhibit expression of key mesenchymal genes to overcome the MET epigenetic barrier of fibroblasts and allow for their successful reprogramming into iPSCs. The gene encoding E-cadherin is activated by *KLF4* expression during reprogramming and is required for generating iPSCs (Chen *et al.*, 2010; Li *et al.*, 2010). In our present study, the expression levels of E-cadherin and *KLF4* in DPCs that were not transduced with reprogramming factors did not increase under

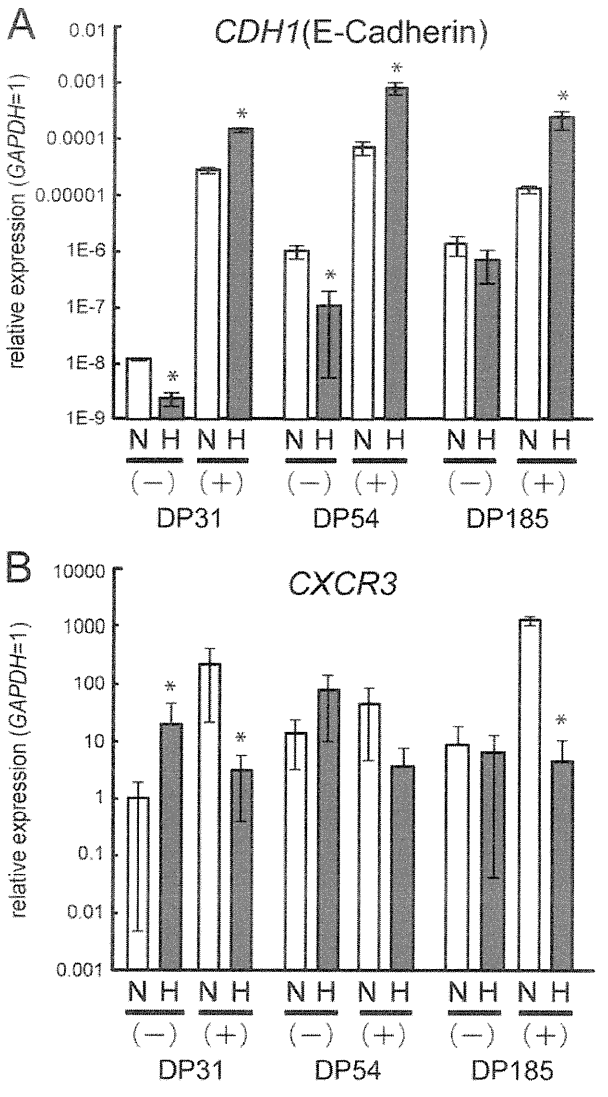

Figure 3. Comparison of the expression levels of *CDH1* (E-cadherin) and *CXCR3* in DPCs exposed to normoxia and hypoxia. DPCs from the three donors were transduced (+) or not (-) as described in "Methods" and then cultured for 6 days under 21% O_2 (N) or 3% O_2 (H). Expression levels of *CDH1* **(A)** and *CXCR3* **(B)** mRNA were assessed by RT-PCR at day 6 post-infection. The mRNA values were divided by those of *GAPDH* and used to calculate expression coefficients. Error bars indicate the SD obtained from triplicate measurements; $*p < .05$ compared with 21% O_2.

hypoxia (*KLF4* data not shown). However, in the presence of reprogramming factors, the expression level of E-cadherin significantly increased. This result in the presence and absence of reprogramming factors is quite interesting because it may indicate that hypoxia affected the early stage of the reprogramming sequence rather than competency of DPCs by changing the expression of E-cadherin and inducing MET.

Microarray analysis revealed that some genes were up-regulated over 10-fold in hypoxia (Table 1). CBLC belongs to the Cbl family of ubiquitin ligases that plays a critical role in protein tyrosine kinase signaling and is exclusively expressed in

epithelial cells, and it may play a role in the MET (Griffiths *et al.*, 2003; Ryan *et al.*, 2012). EGLN3 belongs to the EGLN family of oxygen-sensitive prolyl hydroxylase that controls the degradation of HIF-1α (Epstein *et al.*, 2001). Remarkably, our analysis of microarrays suggested that hypoxia induced changes in the expression levels of several genes encoding chemokines and their receptors (Table 1 and Appendix Figs. 3, 4). Chemokine signaling pathways influence reprogramming target cells toward iPSCs, and the expression of *CCL2*, which encodes a chemokine, dramatically promoted the reprogramming of fibroblasts toward iPSCs (Nagamatsu *et al.*, 2012). Although analysis of our data showed a decrease in *CCL2* expression in hypoxia (Appendix Fig. 4B), the levels of transcription of multiple chemokines and their receptors were altered. Such modulation of chemokine genes may be related to a response of DPCs to inflammation of the teeth, causing signal propagation to the cytokine network (Horst *et al.*, 2011). Interestingly, *CCR4, CCL23*, and *CXCL6*, whose expression levels were altered (Table 1 and Appendix Figs. 3, 4), are expressed at levels 100-fold higher in the odontoblast layer affected by caries (Horst *et al.*, 2011). *IL8*, down-regulated in hypoxia (Table 1), is also an important inflammatory signal mediator. The comparison between up-regulated and down-regulated chemokines and their receptors and examination of downstream signals may reveal the mechanism that underlies the enhanced reprogramming of DPCs observed here.

In the present study, transient hypoxia improved the efficiency of generating iPSCs from DPCs. These conditions differed from those described in a previous report on human DFs. This indicates that complex mechanisms are involved in the effects of hypoxia on the reprogramming process, and that studies conducted *in vitro* must be carefully optimized for each cell type.

ACKNOWLEDGMENTS

We thank the members of the Department of Tissue and Organ Development and the Department of Oral and Maxillofacial Sciences of Gifu University Graduate School of Medicine, and the Center for iPS Cell Research and Application of Kyoto University for their technical help and fruitful discussions. This work was supported by grants from the Ministry of Education, Science, and Culture of Japan, and the JST Yamanaka iPS Cell Project. The authors declare no potential conflicts of interest with respect to the authorship and/or publication of this article.

REFERENCES

Cavallaro U, Christofori G (2004). Cell adhesion and signalling by cadherins and Ig-CAMs in cancer. *Nat Rev Cancer* 4:118-132.

Chen T, Yuan D, Wei B, Jiang J, Kang J, Ling K, *et al.* (2010). E-cadherin-mediated cell-cell contact is critical for induced pluripotent stem cell generation. *Stem Cells* 28:1315-1325.

Chou YF, Chen HH, Eijpe M, Yabuuchi A, Chenoweth JG, Tesar P, *et al.* (2008). The growth factor environment defines distinct pluripotent ground states in novel blastocyst-derived stem cells. *Cell* 135:449-461.

D'Ippolito G, Diabira S, Howard GA, Roos BA, Schiller PC (2006). Low oxygen tension inhibits osteogenic differentiation and enhances stemness of human MIAMI cells. *Bone* 39:513-522.

Epstein AC, Gleadle JM, McNeill LA, Hewitson KS, O'Rourke J, Mole DR, *et al.* (2001). *C. elegans* EGL-9 and mammalian homologs define a family of dioxygenases that regulate HIF by prolyl hydroxylation. *Cell* 107:43-54.

Foja S, Jung M, Harwardt B, Riemann D, Pelz-Ackermann O, Schroeder IS (2013). Hypoxia supports reprogramming of mesenchymal stromal cells via induction of embryonic stem cell-specific microRNA-302 cluster and pluripotency-associated genes. *Cell Reprogram* 15:68-79.

Griffiths EK, Sanchez O, Mill P, Krawczyk C, Hojilla CV, Rubin E, *et al.* (2003). Cbl-3-deficient mice exhibit normal epithelial development. *Mol Cell Biol* 23:7708-7718.

Gronthos S, Mankani M, Brahim J, Robey PG, Shi S (2000). Postnatal human dental pulp stem cells (DPSCs) in vitro and in vivo. *Proc Natl Acad Sci USA* 97:13625-13630.

Gronthos S, Brahim J, Li W, Fisher LW, Cherman N, Boyde A, *et al.* (2002). Stem cell properties of human dental pulp stem cells. *J Dent Res* 81:531-535.

Horst OV, Horst JA, Samudrala R, Dale BA (2011). Caries induced cytokine network in the odontoblast layer of human teeth. *BMC Immunol* 12:9.

Huang X, Ding L, Bennewith KL, Tong RT, Welford SM, Ang KK, *et al.* (2009). Hypoxia-inducible mir-210 regulates normoxic gene expression involved in tumor initiation. *Mol Cell* 35:856-867.

Iida K, Takeda-Kawaguchi T, Tezuka Y, Kunisada T, Shibata T, Tezuka K (2010). Hypoxia enhances colony formation and proliferation but inhibits differentiation of human dental pulp cells. *Arch Oral Biol* 55:648-654.

Li R, Liang J, Ni S, Zhou T, Qing X, Li H, *et al.* (2010). A mesenchymal-to-epithelial transition initiates and is required for the nuclear reprogramming of mouse fibroblasts. *Cell Stem Cell* 7:51-63.

Lin SL, Chang DC, Lin CH, Ying SY, Leu D, Wu DT (2011). Regulation of somatic cell reprogramming through inducible mir-302 expression. *Nucleic Acids Res* 39:1054-1065.

Nagamatsu G, Saito S, Kosaka T, Takubo K, Kinoshita T, Oya M, *et al.* (2012). Optimal ratio of transcription factors for somatic cell reprogramming. *J Biol Chem* 287:36273-36282.

Okita K, Matsumura Y, Sato Y, Okada A, Morizane A, Okamoto S, *et al.* (2011). A more efficient method to generate integration-free human iPS cells. *Nat Methods* 8:409-412.

Packer L, Fuehr K (1977). Low oxygen concentration extends the lifespan of cultured human diploid cells. *Nature* 267:423-425.

Ryan PE, Kales SC, Yadavalli R, Nau MM, Zhang H, Lipkowitz S (2012). Cbl-c ubiquitin ligase activity is increased via the interaction of its RING finger domain with a LIM domain of the paxillin homolog, Hic 5. *PloS One* 7:e49428.

Soncin F, Mohamet L, Eckardt D, Ritson S, Eastham AM, Bobola N, *et al.* (2009). Abrogation of E-cadherin-mediated cell-cell contact in mouse embryonic stem cells results in reversible LIF-independent self-renewal. *Stem Cells* 27:2069-2080.

Suh MR, Lee Y, Kim JY, Kim SK, Moon SH, Lee JY, *et al.* (2004). Human embryonic stem cells express a unique set of microRNAs. *Dev Biol* 270:488-498.

Takahashi K, Tanabe K, Ohnuki M, Narita M, Ichisaka T, Tomoda K, *et al.* (2007). Induction of pluripotent stem cells from adult human fibroblasts by defined factors. *Cell* 131:861-872.

Takeda T, Tezuka Y, Horiuchi M, Hosono K, Iida K, Hatakeyama D, *et al.* (2008). Characterization of dental pulp stem cells of human tooth germs. *J Dent Res* 87:676-681.

Tamaoki N, Takahashi K, Tanaka T, Ichisaka T, Aoki H, Takeda-Kawaguchi T, *et al.* (2010). Dental pulp cells for induced pluripotent stem cell banking. *J Dent Res* 89:773-778.

Watanabe K, Ueno M, Kamiya D, Nishiyama A, Matsumura M, Wataya T, *et al.* (2007). A ROCK inhibitor permits survival of dissociated human embryonic stem cells. *Nat Biotechnol* 25:681-686.

Wilson KD, Venkatasubrahmanyam S, Jia F, Sun N, Butte AJ, Wu JC (2009). MicroRNA profiling of human-induced pluripotent stem cells. *Stem Cells Dev* 18:749-758.

Yoshida Y, Takahashi K, Okita K, Ichisaka T, Yamanaka S (2009). Hypoxia enhances the generation of induced pluripotent stem cells. *Cell Stem Cell* 5:237-241.

Yu CY, Boyd NM, Cringle SJ, Alder VA, Yu DY (2002). Oxygen distribution and consumption in rat lower incisor pulp. *Arch Oral Biol* 47:529-536.